DALTON

Bis(2,2′-bipyridine)ruthenium(II) complexes with imidazo[4,5-*f*][1,10]-phenanthroline or 2-phenylimidazo[4,5-*f*][1,10]phenanthroline‡

Jian-Zhong Wu,[a] Bao-Hui Ye,[a] Lei Wang,[a] Liang-Nian Ji,*,†,[a] Jian-Ying Zhou,[b] Run-Hua Li[b] and Zhong-Yuan Zhou[c]

[a] *Department of Chemistry, Zhongshan University, Guangzhou 510275, China*
[b] *State Key Laboratory of Ultrafast Laser Spectroscopy, Zhongshan University, Guangzhou 510275, China*
[c] *Chengdu Institute of Organic Chemistry, Chinese Academy of Sciences, Chengdu 610041, China*

Imidazo[4,5-*f*]1,10-phenanthroline (ip), 2-phenylimidazo[4,5-*f*][1,10]phenanthroline (pip) and their $(bipy)_2Ru^{2+}$ complexes (bipy = 2,2′-bipyridine) have been synthesized and characterized. The oxidation potentials of $[Ru(bipy)_2(ip)]^{2+}$ and $[Ru(bipy)_2(pip)]^{2+}$ were found to be 1.254 and 1.284 V *vs.* saturated calomel electrode respectively; the reduction of ip and pip appears to be irreversible at *ca.* −0.85 V. The photophysical properties of the complexes were perturbed in the presence of calf thymus DNA. The distinct changes including hypo- or hyper-chromicity at different UV/VIS absorption bands, enhancements of integrated emission intensity and excited-state lifetime, and efficiency of emission quenching by $[Fe(CN)_6]^{4-}$ all indicate the stronger binding affinity to DNA of $[Ru(bipy)_2(pip)]^{2+}$ over that of $[Ru(bipy)_2(ip)]^{2+}$, consistent with the greater planar area and extended π system of the pip ligand. The luminescence of the complexes showed monoexponential decay at any [DNA]:[Ru] ratio. The circular dichroism signals of the dialysates of the racemic complexes against calf thymus DNA suggest that the complexes bind to the DNA with enantioselectivity favouring the Δ isomers. These phenomena all suggest that the complexes bind through intercalation of ip or pip into base pairs. The crystal structure of $[Ru(bipy)_2(ip)][ClO_4]_2\cdot H_2O$ was determined; it contains the planar bidentate ligand ip and two twisted bipy ligands with torsional angles between each bipyridine ring pair of 5.7 and 8.6°.

The interesting chemistry of $[Ru(bipy)_3]^{2+}$ (bipy = 2,2′-bipyridine) has stimulated the preparation and characterization of many new octahedral ruthenium(II) polypyridine complexes in order to elucidate the effects of ligand structures on the redox potentials, excited-state reactivity, luminescence emission, *etc*.[1] This has promoted the development of photochemistry, photophysics, photocatalysis, electrochemistry, photoelectrochemistry, chemi- and electrochemi-luminescence, electron and energy transfer and metallosupramolecular chemistry. Over the past decade the application of a number of such complexes has also received increasing attention as DNA structural probes and mediators of DNA cleavage reactions, utilizing their rich photophysical spectroscopic and electrochemical properties as well as their geometries especially.[2–13] However, unlike some other metal complexes which interact with DNA,[14] no high-resolution structural information precisely reflecting the binding nature of such complexes to nucleic acids has been reported yet. The exact association mechanism involving the prototype complex $[Ru(phen)_3]^{2+}$ (phen = 1,10-phenanthroline) remains an area of vigorous controversy. Barton and co-workers[2a–d,g,h] have proposed *via* a series of experiments that it binds to DNA both by intercalation of one phen ligand in the major groove and through hydrophobic interaction in the minor groove. Satyanarayana *et al.*[7a,b] argued from viscosity measurements that classical intercalation could not be the binding mode. Nordén and co-workers also thought that the binding does not involve intercalation but occurs in the major groove[6a] or minor groove.[6b]

Despite these debates, the opinions of the above researchers are basically consistent[2i–m,6c,7c] about the 'light switch' $[Ru(bipy)_2(dppz)]^{2+}$ or $[Ru(phen)_2(dppz)]^{2+}$ (dppz = dipyrido[3,2-*a*:2′,3′-*c*]phenazine). The two complexes bind avidly to DNA by 'classical' intercalation of the elongated planar dppz ligand into the DNA base pairs.

All the studies[2–13] revealed that modification of the ligands would lead to subtle or substantial changes in the binding modes, location and affinities, giving chances to explore various valuable conformation- or site-specific DNA probes and potential chemotherapeutical agents. In general, extension of the planarity at the 5,6 sites of phen will increase the strength of interaction of the complexes with DNA. We report here an investigation of the spectral and electrochemical properties of two $(bipy)_2Ru^{2+}$ complexes with imidazo[4,5-*f*][1,10]phenanthroline (ip) or 2-phenylimidazo[4,5-*f*][1,10]phenanthroline (pip). Their association with calf thymus DNA was studied by electronic absorption, emission quenching, excited-state lifetime and circular dichroism measurements. The structure of $[Ru(bipy)_2(ip)]^{2+}$ was determined by using single-crystal diffraction techniques and may well, together with the structure of pip previously reported,[15] account for the DNA binding behaviour. In each complex, two bipy are used as co-complexation ligands with ip or pip, because bipy has been previously demonstrated to be at best only minimally efficient at inducing intercalative binding with DNA,[2b,f,i,3a,b] allowing us to focus on the influences of ip and pip on the interaction.

Experimental

Syntheses

The compounds *cis*-$[Ru(bipy)_2Cl_2]\cdot 2H_2O$[16] and 1,10-phenanthroline-5,6-dione[6c] were prepared by the literature routes. Other materials were commercially available and of reagent grade.

ip. A mixture of formaldehyde (3.5 mmol, 0.26 cm^3 of 36–38% solution) or hexamethylenetetramine (5 mmol, 0.70 g),

† E-mail:cesjln@zsulink.zsu.edu.cn
‡ *Supplementary data available* (No. SUP 57223, 3 pp.): NMR data. See Instructions for Authors, *J. Chem. Soc., Dalton Trans.*, 1997, Issue 1.

1,10-phenanthroline-5,6-dione (2.5 mmol, 0.525 g), ammonium acetate (50 mmol, 3.88 g) and glacial acetic acid (7 cm^3) was refluxed for about 1 h then cooled to room temperature and diluted with water (*ca.* 25 cm^3). Dropwise addition of concentrated aqueous ammonia gave a yellow precipitate, which was collected and washed with water. The crude product in ethanol was purified by silica gel filtration (60–100 mesh, ethanol). The principal yellow band was collected. Slow evaporation of the reduced solution yielded a yellow crystalline solid (0.47 g, 85%), m.p. >310 °C (Found: C, 70.6; H, 3.6; N, 25.2. $C_{13}H_8N_4$ requires C, 70.9; H, 3.7; N, 25.4%). $\tilde{\nu}_{max}/cm^{-1}$ 3437m, 3114s, 1616m, 1419m, 1391m, 800s and 737s. λ_{max}/nm ($\varepsilon/dm^3\ mol^{-1}\ cm^{-1}$) (EtOH) 203 (18 800), 242 (22 400), 248 (23 000) and 282 (14 900).

pip·EtOH. This compound was synthesized similarly, with benzaldehyde (3.5 mmol, 0.35 cm^3) in place of formaldehyde. It crystallized with one molecule ethanol. Yield 89%, m.p. >310 °C (Found: C, 73.7; H, 5.2; N, 16.5. $C_{19}H_{12}N_4{\cdot}C_2H_5OH$ requires C, 73.7; H, 5.3; N, 16.4%). $\tilde{\nu}/cm^{-1}$ 3420m, 3114s, 1609m, 1433m, 1398m, 807s and 744s. λ_{max}/nm ($\varepsilon/dm^3\ mol^{-1}\ cm^{-1}$) (EtOH) 195 (28 800), 222 (24 500), 273 (32 300) and 288 (29 100).

$[Ru(bipy)_2(ip)][ClO_4]_2{\cdot}H_2O$. A mixture of $[Ru(bipy)_2Cl_2]{\cdot}2H_2O$ (0.5 mmol, 0.261 g), ip (0.5 mmol, 0.110 g), methanol (20 cm^3) and water (10 cm^3) was refluxed under argon for 2 h to give a clear red solution and then most of the methanol solvent was removed under reduced pressure. Upon cooling, the solution was chromatographed on a Sephadex C-25 column (Na^+ form, 10 g) with 0.1 mol dm^{-3} sodium chloride in acetone–water (4:1 v/v) as eluent. Dropwise addition of a saturated solution of sodium perchlorate gave red crystals (0.266 g, 62%) (Found: C, 46.1; H, 3.2; N, 1.32. $C_{33}H_{26}Cl_2N_8O_9Ru$ requires C, 46.6; H, 3.1; N, 13.2%). $\tilde{\nu}_{max}/cm^{-1}$ 3450w (br), 3070w, 1625w, 1601m, 1444m, 1361m, 1099vs, 932m, 804m, 766s, 725m, 621s and 417w. λ_{max}/nm ($\varepsilon/dm^3\ mol^{-1}\ cm^{-1}$) (water) 250 (60 000), 280 (74 000) and 455 (16 100).

$[Ru(bipy)_2(pip)][ClO_4]_2{\cdot}3H_2O$. This complex was prepared similarly, using pip·EtOH in place of ip. Yield 65% (Found: C, 48.6; H, 3.2; N, 11.5. $C_{39}H_{34}Cl_2N_8O_{11}Ru$ requires C, 48.6; H, 3.6; N, 11.6%). $\tilde{\nu}_{max}/cm^{-1}$ 3421w (br), 3070w, 1622w, 1601m, 1444m, 1361m, 1091vs, 930m, 806m, 763s, 720m, 623s and 420w. λ_{max}/nm ($\varepsilon/dm^3\ mol^{-1}\ cm^{-1}$) (water) 244 (37 900), 254 (37 100), 283(113 800) and 458 (20 100).

CAUTION: solid perchlorate salts are potentially explosive and should be handled with care.

Physical measurements

All the experiments involving the interaction of the complexes with DNA were conducted in deionized water buffer containing tris(hydroxymethyl)aminomethane (Tris, 5 mmol dm^{-3}) and sodium chloride (50 mmol dm^{-3}) and adjusted to pH 7.0 with hydrochloric acid. Solutions of calf thymus DNA gave ratios of UV absorbance at 260 and 280 nm of *ca.* 1.8–1.9:1, indicating that the DNA was sufficiently free of protein.[17] The DNA concentration per nucleotide was determined spectrophotometrically by assuming ε_{260} 6600 $dm^3\ mol^{-1}\ cm^{-1}$.[18]

Microanalyses (C, H and N) were carried out with a Perkin-Elmer 240Q elemental analyser. Infrared spectra were recorded on a Nicolet 170SX-FTIR spectrometer as KBr discs, UV/VIS spectra on a Shimadzu MPS-2000 spectrophotometer and NMR spectra on a Bruker ARX-300 NMR spectrometer with $(CD_3)_2SO$ as solvent for the pro-ligands or CD_3CN for the complexes at room temperature (^1H at 300.13 MHz, ^{13}C at 75.47 MHz with wide-band proton decoupling). The two-dimensional NMR experiment was carried out with the standard program.

Cyclic voltammetry was performed on an EG&G PAR 273 polarographic analyser and 270 universal programmer. The supporting electrolyte was 0.1 mol dm^{-3} tetraethylammonium perchlorate in acetonitrile freshly distilled from phosphorus pentaoxide and deaerated by purging with nitrogen. A standard three-electrode system was used comprising a platinum microcylinder working electrode, platinum-wire auxiliary electrode and a saturated calomel reference electrode (SCE).

The luminescence lifetime measurements were done with an excimer laser (Lambda Physics EMG 201MSC)–pumped dye laser (Lambda Physics model FL2002) system. The nominal pulse width and the linewidth of the dye-laser output were 10 ns and 0.18 cm^{-1}, respectively. The excitation wavelength was fixed at 455 nm. The emission of a sample was collected by two lenses into a monochromator, detected by a photomultiplier and processed by a Boxcar Averager (EG&G model 162) in line with a microcomputer.

Equilibrium dialysis were conducted at room temperature with 5 cm^3 of calf thymus DNA (1.06 mmol dm^{-3}) sealed in a dialysis bag and 10 cm^3 of the complex (0.6 mmol dm^{-3}) outside the bag and the system agitated on a shaker bath. After 2 d the circular dichroism (CD) spectrum of the dialysate outside the bag was measured on a JASCO J-20C spectropolarimeter.

Crystallography

Crystal data and data collection parameters. $C_{33}H_{26}Cl_2N_8O_9Ru$, $M = 850.6$, monclinic, space group $P2_1/c$, $a = 13.1410(10)$, $b = 19.4840(10)$, $c = 14.1700(10)$ Å, $\beta = 109.210(0)°$, $U = 3425.9(5)$ $Å^3$, $T = 294$ K, $Z = 4$, λ(Mo-Kα) = 0.710 73 Å, $D_c = 1.649$ g cm^{-3}, $F(000) = 1720$, $\mu = 0.684$ mm^{-1}, red prism with dimensions 0.22 × 0.28 × 0.32 mm. Siemens P4 diffractometer, ω scans, data collection range $3.0 < 2\theta < 48.0°$, $-1 \leqslant h \leqslant 15$, $-1 \leqslant k \leqslant 23$, $-16 \leqslant l \leqslant 16$; 6560 reflections measured, 5356 unique ($R_{int} = 0.0185$) and 3568 observed with $F > 4.0\sigma(F)$ which were used for structure solution.

Structure solution and refinement. The structure was solved by direct methods and subsequent Fourier-difference syntheses, and refined anisotropically on F by full-matrix least-squares techniques using the SHELXTL PC program package.[19] Hydrogen atoms were included using a riding model. Semi-empirical absorption corrections (ψ scan) were applied.[19] Convergence was reached at $R = 0.0546$, $R' = 0.0815$ with $w^{-1} = \sigma^2(F) + 0.0010F^2$. Largest difference peak 0.71 e $Å^{-3}$

Atomic coordinates, thermal parameters, and bond lengths and angles have been deposited at the Cambridge Crystallographic Data Centre (CCDC). See Instructions for Authors, *J. Chem. Soc., Dalton Trans.*, 1997, Issue 1. Any request to the CCDC for this material should quote the full literature citation and the reference number 186/419.

Results and Discussion

NMR spectra

The ^1H and ^{13}C NMR data and assignments for the pro-ligands and the complexes have been deposited together with the ^1H–^{13}C correlation (COSY) spectra of the complexes (SUP 57223). The proton on the nitrogen atom of the imidazole, resonating at *ca.* δ 13.5 for ip and pip as a broad singlet and unobserved for $[Ru(bipy)_2(ip)]^{2+}$ and $[Ru(bipy)_2(pip)]^{2+}$, exchanges quickly between the two nitrogens of the imidazole ring, characteristic of an active proton. So the pro-ligands and the complexes all exhibit C_{2v} symmetry in NMR experiments. As a consequence, in the complexes the two bipy ligands and the two halves of ip or pip are chemically and magnetically equivalent, respectively. However, the two pyridine rings of each bipy are not, due to the distinct shielding influences of the adjacent bipy and ip (or pip), leading to eight signals corre-

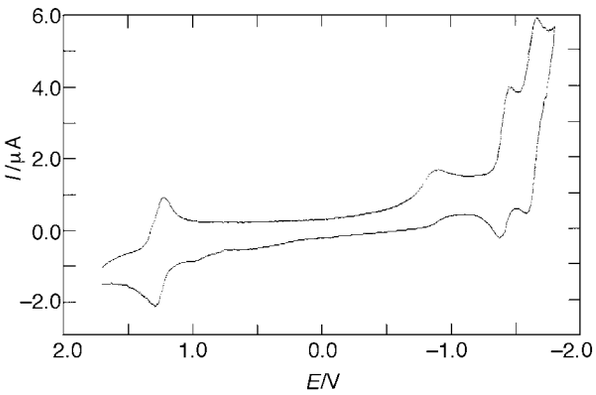

Fig. 1 Cyclic voltammogram of $[Ru(bipy)_2(ip)]^{2+}$

sponding to the bipy protons: one set of four is associated with the pyridine ring near the ip or pip, the other set of four is associated with the pyridine ring near the other bipy. Since the shielding effect of ip or pip is obviously greater than that of bipy, the chemical shifts of the latter protons are greater than those of the former.

Electrochemistry

Each complex exhibits well shaped oxidation (one) and reduction (two) waves in the sweep range from −1.8 to +1.7 V, the half-wave potentials being 1.254, −1.419 and −1.659 V *vs.* SCE for $[Ru(bipy)_2(ip)]^{2+}$ and 1.284, −1.410 and −1.618 V for $[Ru(bipy)_2(pip)]^{2+}$. The anodic and cathodic peak separations vary from 58 to 76 mV and are nearly scan rate independent, indicating that the processes are reversible one-electron transfers. A small, poorly shaped reduction wave appears at *ca.* −0.85 V, as shown in Fig. 1 for $[Ru(bipy)_2(ip)]^{2+}$.

Oxidation of the complexes involves removal of an electron from the d_π orbital of Ru^{II}, while reduction involves transfer of an electron to the ligand-centred orbitals. The attachment of a phenyl ring to the ip moiety expands the π delocalization and thus decreases the σ-donor capacity of pip. This leads to an increase in the formal charge on ruthenium in $[Ru(bipy)_2(pip)]^{2+}$, and in turn stabilizes the metal d_π orbital directly and the ligand π* orbital indirectly through charge interactions. Subsequent d_π–π* back bonding further stabilizes the metal d_π orbital but destabilizes the ligand π* orbital.[20] So the oxidation response of $[Ru(bipy)_2(pip)]^{2+}$ shifts positively by 30 mV to that of $[Ru(bipy)_2(ip)]^{2+}$. The first reduction, usually expected to involve the ligand having the most stable lowest unoccupied molecular orbital (LUMO),[20–22] obviously ip or pip here, appears irreversible and makes the comparison between the two complexes difficult. The later two successive reductions are characteristic of the two bipy ligands.[1a,b,22]

Crystal structure

The molecular structure of $[Ru(bipy)_2(ip)][ClO_4]_2\cdot H_2O$ has been confirmed by single-crystal X-ray diffraction analysis. An ORTEP[23] view of the cation is illustrated in Fig. 2. Selected bond lengths and angles are given in Table 1, some dihedral angles in Table 2. The overall structure of the cation is that of a distorted octahedron, with a bite angle of 78.9° averaged over the three bidentate ligands. The mean Ru–N (bipy) distance is 2.055 Å, similar to that found in $[Ru(bipy)_3]^{2+}$ (2.056 Å).[24] The Ru–N (ip) distance, 2.070 Å, is similar to that of Ru–N (phen) (2.069 Å) in $[Ru(bipy)_2(phen)]^{2+}$,[25] implying that imidazole conjugation has little influence on the electron distribution.

The complex has notable torsional angles between the pyridine pairs of each bipy ligand, 5.7 and 8.6°, in comparison with those of $[Ru(bipy)_3]^{2+}$ (2.2°),[24] $[Ru(bipy)_2Cl_2]^{2+}$ (1.3°),[26a] $[Ru(bipy)_2(glyO)]^{+}$ (glyO = glycinate) (1.4 and 7.4°),[26b] $[Ru(bipy)_2(NCS)_2]^{2+}$ (4.5°),[26c] $[Ru(bipy)_2(py)_2]^{2+}$ (py = pyridine) (5.7°),[26d] $[Ru(bipy)_2\{C_6H_4(NH_2)_2\text{-}1,2\}]^{2+}$ (11.41 and 8.04°),[26e] $[Ru(bipy)_2(tmbipy)]^{2+}$ [tmbipy = 3,3,3′,3′-tetramethylenebis(bipyridine)] (1.4 and 7.2°),[26f] $[Ru(bipy)_2(phen)]^{2+}$ (6.4 and 10.3°)[25] and $[Ru(bipy)_2(mphen)]^{2+}$ (mphen = 5-methyl-1,10-phenanthroline) (1.9 and 12.3°).[25] On the contrary, the ip ligand is planar with an average deviation from the least-squares plane of 0.0340 Å. So it possesses intercalating potential for DNA adjacent base pairs, whereas bipy does not, as evident with other $[Ru(bipy)_2L]^{2+}$-type DNA-binding agents.[2b,f,i,3a,b] Stacking interactions between the ip ligands are observed in the crystal unit.

Although single crystals of $[Ru(bipy)_2(pip)]^{2+}$ have not yet been obtained, the crystal structure of pip is known.[15] The

Table 1 Selected bond lengths (Å) and angles (°) for $[Ru(bipy)_2(ip)][ClO_4]_2\cdot H_2O$

Ru–N(1)	2.056(4)	Ru–N(2)	2.062(4)
Ru–N(3)	2.055(3)	Ru–N(4)	2.047(4)
Ru–N(5)	2.069(4)	Ru–N(6)	2.070(3)
N(1)–Ru–N(2)	78.9(1)	N(1)–Ru–N(3)	95.5(1)
N(2)–Ru–N(3)	89.7(1)	N(1)–Ru–N(4)	170.6(1)
N(2)–Ru–N(4)	94.1(1)	N(3)–Ru–N(4)	77.9(1)
N(1)–Ru–N(5)	96.2(1)	N(2)–Ru–N(5)	173.2(2)
N(3)–Ru–N(5)	95.6(1)	N(4)–Ru–N(5)	91.2(1)
N(1)–Ru–N(6)	90.8(1)	N(2)–Ru–N(6)	95.3(1)
N(3)–Ru–N(6)	172.6(2)	N(4)–Ru–N(6)	96.2(1)
N(5)–Ru–N(6)	79.9(1)	Ru–N(1)–C(1)	126.5(3)
Ru–N(1)–C(5)	115.6(2)	Ru–N(2)–C(6)	115.9(2)
Ru–N(2)–C(10)	127.5(3)	Ru–N(3)–C(11)	126.0(3)
Ru–N(3)–C(15)	117.1(2)	Ru–N(4)–C(16)	116.8(2)
Ru–N(4)–C(20)	125.4(3)	Ru–N(5)–C(21)	126.8(3)
Ru–N(5)–C(33)	114.3(2)	Ru–N(6)–C(31)	129.6(3)
Ru–N(6)–C(32)	113.4(2)		

Table 2 Some dihedral angles of $[Ru(bipy)_2(ip)][ClO_4]_2\cdot H_2O$

Plane	Atoms	Dihedral angle/°
1	N(1), N(2), C(1)–C(10)	
2	N(3), N(4), C(11)–C(20)	1 and 2 86.2
3	N(5)–N(8), C(21)–C(26)	1 and 3 96.9, 2 and 3 96.6
4	N(1), C(1)–C(5)	
5	N(2), C(6)–C(10)	4 and 5 5.7
6	N(3), C(11)–C(15)	
7	N(4), C(16)–C(20)	6 and 7 171.4
8	N(5), N(6), C(21)–C(25), C(27)–C(33)	3 and 8 0.9
9	N(7), N(8), C(25)–C(27)	8 and 9 1.6
10	N(3), N(4), Ru	1 and 10 3.6
11	N(3), N(4), Ru	2 and 11 5.9
12	N(5), N(6), Ru	3 and 12 3.3

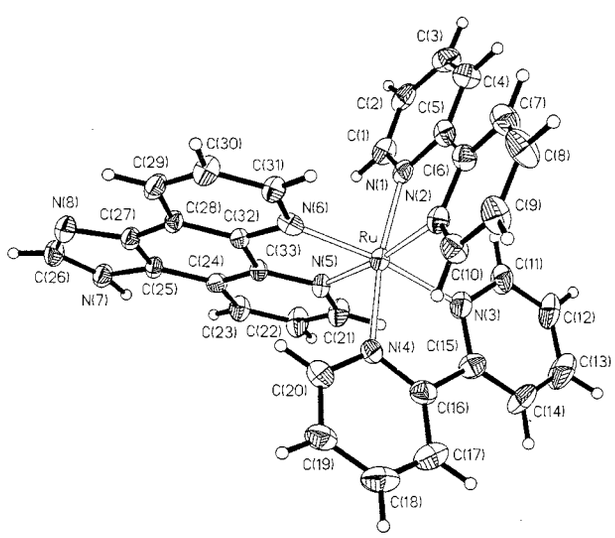

Fig. 2 An ORTEP view of $[Ru(bipy)_2(ip)]^{2+}$

phenyl ring is almost strictly coplanar with the ip moiety. So pip has a larger planar area and would be expected to stack with DNA base pairs more strongly. This is unlike $[Ru(dpphen)]^{2+}$ (dpphen = 4,7-diphenyl-1,10-phenanthroline), in which the phenyl groups are skew to the phen moieties.[27] It binds to B-DNA only with one phenyl group of one dpphen in the minor groove, leaving the other phenyl group and another non-intercalating dpphen aligned along the major groove, as predicted by molecular model construction.

Electronic absorption spectra

The electronic absorption spectra of the two complexes, unchanged between water and Tris buffer, are similar in shape to that of $[Ru(bipy)_3]^{2+}$.[1a–c] The metal d_π to ligand π^* charge-transfer m.l.c.t. band in the visible region appears at 452, 455 and 458 nm with a less-intense shoulder at shorter wavelength for $[Ru(bipy)_3]^{2+}$, $[Ru(bipy)_2(ip)]^{2+}$ and $[Ru(bipy)_2(pip)]^{2+}$, respectively. The bathochromic shift trend is in accord with the extension of the corresponding π framework. However, these shifts are much less dramatic than those of some other $[Ru(bipy)_2L]^{2+}$ complexes (L is a polypyridine ligand with a more extended π-electron system than that of bipy),[22c,d] which even exhibit splitting of the m.l.c.t. absorption assignable individually to $Ru(d_\pi)$–bipy(π*) and $Ru(d_\pi)$–L(π*). Two comparable examples are $[Ru(bipy)_2(dppz)]^{2+}$ [20] and $[Ru(dppz)_3]^{2+}$,[28] which exhibit m.l.c.t. absorption at 448 and 455 nm respectively despite the large extent of π delocalization of the dppz ligand. The authors ascribed these to the strong π-accepting phenazine site being only slightly coupled electronically to the ruthenium core and so the complexes show bichromophoric character of $Ru('bipy')_3^{2+}$ and phenazine. The complexes studied here are believed to resemble these with a benzimidazole or 2-phenylbenzimidazole site coupled to ruthenium electronically but not strongly. This is supported by the similar Ru–N (ip) length to that of Ru–N (phen) (see above). Regarding the correlation between the crystal structure and the visible m.l.c.t. of $[Ru(bipy)_2(diimine)]^{2+}$, it seems that if Ru–N (diimine) is significantly short the corresponding m.l.c.t. will occur with markedly low energy,[26e,29] otherwise it will be only around 450 nm [25,26f] similar to that of $[Ru(bipy)_3]^{2+}$

In the UV region, the intense, fairly narrow band at 280 or 283 nm for $[Ru(bipy)_2(ip)]^{2+}$ or $[Ru(bipy)_2(pip)]^{2+}$ respectively is attributable to internal π to π* transitions of the co-ordinated groups, with the magnitude also in accord with the π extension. However, the assignments of the higher energy absorption appearing as a slightly shouldered intense band at 250 nm for $[Ru(bipy)_2(ip)]^{2+}$, or as two separate weaker bands at 254 and 244 nm for $[Ru(bipy)_2(pip)]^{2+}$, m.l.c.t.[1a–c] or to π–π*[30] remain ambiguous.

The application of electronic absorption spectroscopy in DNA-binding studies of ruthenium polypyridines is one of the most useful techniques.[2a,f,3a,4a,b] However, previous studies monitored only the visible m.l.c.t. band, which showed that the presence of DNA resulted in hypochromism, due to the intercalative mode involving a strong stacking interaction between an aromatic chromophore and the base pairs of DNA. The extent of the hypochromism commonly parallels the intercalative binding strength. As a corollary to this, we believe that the ultraviolet transition bands should display similar behaviour. The absorption spectra of the complexes in the absence and the presence of calf thymus DNA (with subtraction of the DNA absorbance for the latter) are illustrated in Fig. 3. The visible m.l.c.t. band of $[Ru(bipy)_2(ip)]^{2+}$ is decreased by 15.5%, that of $[Ru(bipy)_2(pip)]^{2+}$ by 21.9%. So the latter complex is more strongly intercalative to DNA base pairs than is the former. This is just the expected result on the basis that pip possesses a greater planar area and extended π system and hence higher hydrophobicity than that of ip, which would lead to pip penetrating more deeply into, and stacking more strongly

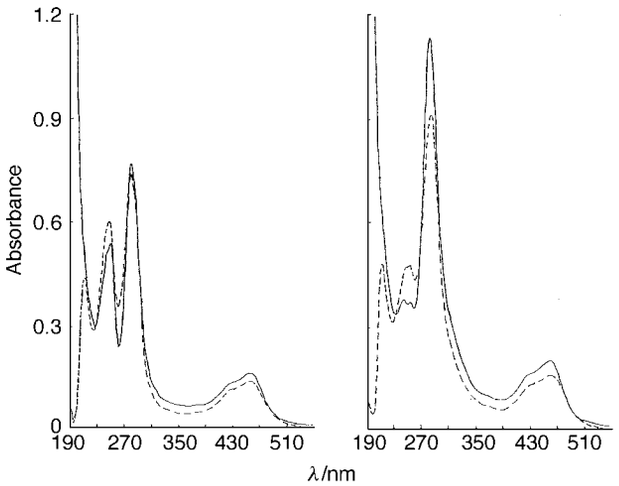

Fig. 3 Electronic absorption spectra of $[Ru(bipy)_2(ip)]^{2+}$ (left) and $[Ru(bipy)_2(pip)]^{2+}$ (right) with no DNA (—) and [DNA] : [Ru] = 26 : 1 (---) with subtraction of the DNA absorbance. [Ru] = 10 μmol dm^{-3}

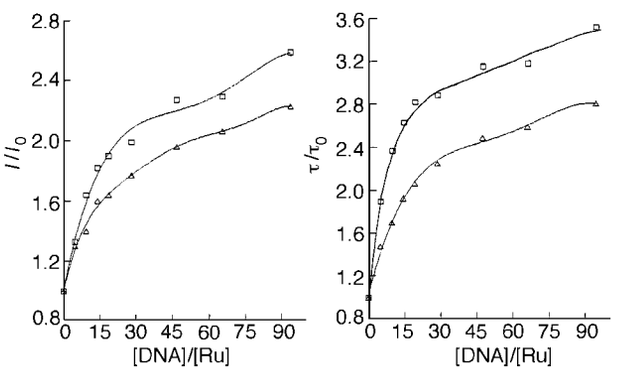

Fig. 4 Plots of relative integrated emission intensity (left) and excited-state lifetime (right) *versus* [DNA] : [Ru] ratio for $[Ru(bipy)_2(ip)]^{2+}$ (△) and $[Ru(bipy)_2(pip)]^{2+}$ (□)

with, the DNA base pairs. Similarly, concerning the π–π* transition at about 280 nm, $[Ru(bipy)_2(ip)]^{2+}$ shows slight hypochromicity (3.8%), whereas $[Ru(bipy)_2(pip)]^{2+}$ shows 20.0%. The bands around 250 nm exhibit hyperchromicities of 11.5 and 28.0% respectively. We infer that these m.l.c.t. or π–π* bands are predominantly based on bipy. The non-intercalation character of bipy leads to contrary changes, but the extent of hyperchromicity is consistent with the intercalative ability of ip and pip.

Luminescence spectroscopic studies

The complexes $[Ru(bipy)_2(ip)]^{2+}$ and $[Ru(bipy)_2(pip)]^{2+}$ can emit luminescence in Tris buffer at ambient temperature in a manner similar to $[Ru(bipy)_3]^{2+}$, with maxima at 625 and 615 nm, respectively. Upon addition of calf thymus DNA, enhancements in both integrated emission intensities and lifetimes of the complexes were observed, monitored by time-resolved techniques at the respective emission maxima, as shown in Fig. 4. The extent of either type of enhancement increases on going from $[Ru(bipy)_2(ip)]^{2+}$ to $[Ru(bipy)_2(pip)]^{2+}$ consistent with the intercalation mode. Since pip is expected to insert more deeply and strongly than ip, it would induce at least two greater changes which would lead to enhancements in emission intensity and lifetime. First, the hydrophobic environment inside the DNA helix reduces the accessibility of water molecules to the complex; secondly, the complex mobility is restricted at the binding site and so the vibrational modes of relaxation decrease.

Steady-state emission quenching experiments using

$[Fe(CN)_6]^{4-}$ as quencher further support the above proposal. As illustrated in Fig. 5, in the absence of DNA, $[Ru(bipy)_2(ip)]^{2+}$ and $[Ru(bipy)_2(pip)]^{2+}$ were efficiently quenched by $[Fe(CN)_6]^{4-}$ resulting in two strictly linear Stern–Volmer plots. However, the presence of DNA made the plots drastically curved. This can be explained by repulsion of the highly anionic $[Fe(CN)_6]^{4-}$ by the DNA polyanion which hinders quenching of the emission of the bound complex.[2b,c] The slope can therefore be taken as a measure of binding affinity, a larger value corresponding to poorer protection and lower binding. So $[Ru(bipy)_2(pip)]^{2+}$ binds more tightly than $[Ru(bipy)_2(ip)]^{2+}$, consistent with a stronger penetrating ability of pip than that of ip.

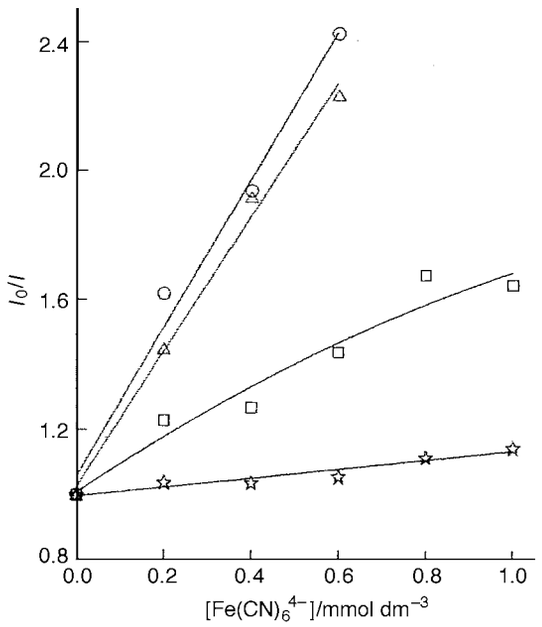

Fig. 5 Emission quenching of the complexes with increasing concentrations of $[Fe(CN)_6]^{4-}$. [Ru] = 2 μmol dm^{-3}, [DNA] : [Ru] = 40 : 1. (○) Free $[Ru(bipy)_2(ip)]^{2+}$, (△) free $[Ru(bipy)_2(pip)]^{2+}$, (□) $[Ru(bipy)_2(ip)]^{2+}$ + DNA, (☆) $[Ru(bipy)_2(pip)]^{2+}$ + DNA

We were surprised to find in the lifetime measurements that for the two complexes all the decay profiles were monoexponential at any [DNA] : [Ru] ratio. As an example, plots of emission intensity and its natural logarithm *vs.* time at [DNA] : [Ru] = 47 : 1 for $[Ru(bipy)_2(pip)]^{2+}$ are shown in Fig. 6. In their studies of *rac*-$[Ru(phen)_3]^{2+}$–DNA binding, Barton *et al.*[2c] resolved the decay curve to obtain two lifetimes, one longer with a pre-exponential weighting factor of *ca.* 24.5% attributable to the intercalative component, another shorter of *ca.* 70% corresponding to the surface-bound component, and they thought that the third component, *i.e.* the free form, can result in time averaging of the two lifetimes through a fast exchange. However, in another experiment[2g] the weighting factor of the longer lifetime was 71 or 61% for Δ- or Λ-$[Ru(phen)_3]^{2+}$, that of the shorter one 29 or 39% for Δ or Λ, respectively. For the 'light switch' $[Ru(phen)_2(dppz)]^{2+}$,[2j,k] two lifetimes were also found, which were assigned to two intercalative modes but no surface-binding mode; the longer lifetime corresponds to a perpendicular mode, where the Ru–dppz axis lies perpendicular to the base-pair long axis, the shorter to a side-on mode with the Ru–dppz axis more in line with the base-pair long axis. Tysoe *et al.*[4b] investigated the binding modes of Δ- and Λ-$[Ru(bipy)_2(pzp)]^{2+}$ (pzp = pyrazino[2,3-*f*][4,7]phenanthroline) with calf thymus DNA and also got two types of lifetime and assigned them similarly to $[Ru(phen)_3]^{2+}$. The pre-exponential factors were 85 or 73% with the longer for Δ or Λ, 15 or 27% with the shorter for Δ or Λ, respectively. We note that the ratio of the intercalative component to the surface-bound one for this complex is higher than of $[Ru(phen)_3]^{2+}$. Compared to these results, we speculate that both $[Ru(bipy)_2(ip)]^{2+}$ and $[Ru(bipy)_2(pip)]^{2+}$ bind to calf thymus DNA through an intercalation mode, with ip or pip at least partially within the DNA base pairs.

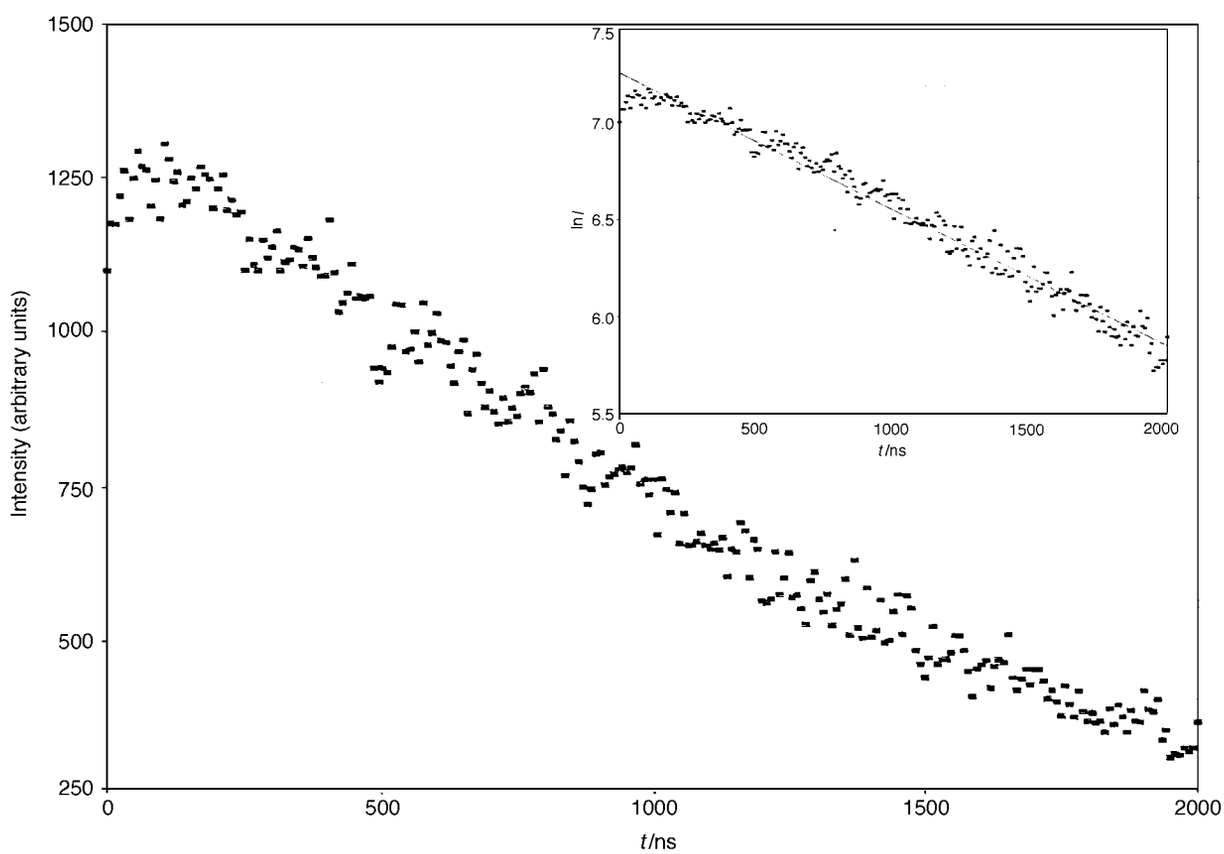

Fig. 6 Typical emission decay profile and the natural logarithm of emission intensity *versus* time (inset) for $[Ru(bipy)_2(pip)]^{2+}$ at [Ru] = 10 μmol dm^{-3}, [DNA] : [Ru] = 47 : 1

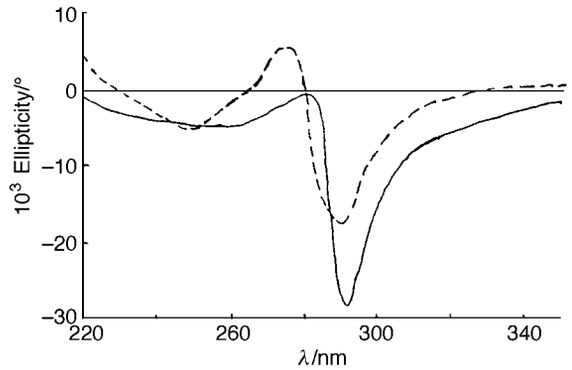

Fig. 7 The CD spectra of the dialysates of $[Ru(bipy)_2(ip)]^{2+}$ (---) and $[Ru(bipy)_2(pip)]^{2+}$ (—) after 48 h of dialysis against calf thymus DNA. [Ru] = 0.6, [DNA] = 1.06 mmol dm^{-3}

Enantioselective binding studies

According to the insertion model proposed by Barton and co-workers,[2a,d,h] the Δ enantiomer of the complex, a right-handed propeller-like structure, will display a greater affinity than the Λ enantiomer for the right-handed calf thymus DNA helix, due to appropriate steric matching. This discrimination can be observed *via* equilibrium dialysis experiments and provide strong evidence in support of intercalation.

The circular dichroism spectra in the UV region of $[Ru(bipy)_2(ip)]^{2+}$ and $[Ru(bipy)_2(pip)]^{2+}$ after their racemic solutions had been dialysed against calf thymus DNA are shown in Fig. 7 (the signals in the visible region are too weak and not shown). The presence of CD signals indicates enrichment of the isomer which binds less favourably to the DNA. The spectra of the dialysates of $[Ru(bipy)_2(ip)]^{2+}$ and $[Ru(bipy)_2(pip)]^{2+}$ are very similar and also like that of the analogous $[Ru(bipy)_2(pzp)]^{2+}$ dialysate[4a] proved to be Λ configuration,[4b] so we conclude that the absolute configurations of the dialysates of $[Ru(bipy)_2(ip)]^{2+}$ and $[Ru(bipy)_2(pip)]^{2+}$ are also Λ. Such a comparison and assumption previously helped Barton and co-workers[2f] to determine the absolute configurations of many ruthenium complexes containing phen derivatives in equilibrium dialysis experiments. Therefore, the Δ isomers of $[Ru(bipy)_2(ip)]^{2+}$ and $[Ru(bipy)_2(pip)]^{2+}$ preferentially bind to calf thymus DNA, as anticipated from the intercalative binding model.

Acknowledgements

We are grateful to the National Natural Science Foundation of China, the State Key Laboratory of Coordination Chemistry in Nanjing University and Lanzhou Institute of Chemical Physics of the Chinese Academy of Sciences for their financial support.

References

1 (*a*) K. Kalyanasundaram, *Coord. Chem. Rev.*, 1982, **46**, 159; (*b*) A. Juris, V. Balzani, F. Barigelletti, S. Campagna, P. Belser and A. von Zelewsky, *Coord. Chem. Rev.*, 1988, **84**, 85; (*c*) E. A. Seddon and K. R. Seddon, *The Chemistry of Ruthenium*, Elsevier, Amsterdam, 1984, ch. 15; (*d*) R. Krause, *Struct. Bonding* (*Berlin*), 1987, **67**, 1; (*e*) E. C. Constable, *Adv. Inorg. Chem.*, 1989, **34**, 1; (*f*) E. C. Constable, *Prog. Inorg. Chem.*, 1994, **42**, 67.

2 (*a*) J. K. Barton and A. L. Raphael, *J. Am. Chem. Soc.*, 1984, **106**, 2172; (*b*) C. V. Kumar, J. K. Barton and N. J. Turro, *J. Am. Chem. Soc.*, 1985, **107**, 5518; (*c*) J. K. Barton, J. M. Goldberg, C. V. Kumar and N. J. Turro, *J. Am. Chem. Soc.*, 1986, **108**, 2081; (*d*) J. K. Barton, *Science*, 1986, **233**, 727; (*e*) M. D. Purugganan, C. V. Kumar, N. J. Turro and J. K. Barton, *Science*, 1988, **241**, 164; (*f*) A. M. Pyle, J. P. Rehmann, R. Meshoyrer, C. V. Kumar, N. J. Turro and J. K. Barton, *J. Am. Chem. Soc.*, 1989, **111**, 3051; (*g*) J. P. Rehmann and J. K. Barton, *Biochemistry*, 1990, **29**, 1701; (*h*) A. M. Pyle and J. K. Barton, *Prog. Inorg. Chem.*, 1990, **38**, 413; (*i*) A. E. Friedman, C. V. Kumar, N. J. Turro and J. K. Barton, *Nucleic Acids Res.*, 1991, **19**, 2595; (*j*) R. M. Hartshorn and J. K. Barton, *J. Am. Chem. Soc.*, 1992, **114**, 5919; (*k*) Y. Jenkins, A. E. Friedman, N. J. Turro and J. K. Barton, *Biochemistry*, 1992, **31**, 10 809; (*l*) C. M. Dupurer and J. K. Barton, *J. Am. Chem. Soc.*, 1994, **116**, 10 286; (*m*) C. Turro, S. H. Bossmann, Y. Jenkins, J. K. Barton and N. J. Turro, *J. Am. Chem. Soc.*, 1995, **117**, 9026.

3 (*a*) J. M. Kelly, A. B. Tossi, D. J. McConnell and C. Ohuigin, *Nucleic Acids Res.*, 1985, **13**, 6017; (*b*) A. B. Tossi and J. M. Kelly, *Photochem. Photobiol.*, 1989, **49**, 545; (*c*) F. de Buyl, A. Kirsch-De Mesmaeker, A. B. Tossi and J. M. Kelly, *J. Photochem. Photobiol. A: Chem.*, 1991, **60**, 27; (*d*) J.-P. Lecomte, A. Kirsch-De Mesmaeker, M. M. Feeney and J. M. Kelly, *Inorg. Chem.*, 1995, **34**, 6481.

4 (*a*) R. J. Morgan, S. Chatterjee, A. D. Baker and T. C. Strekas, *Inorg. Chem.*, 1991, **30**, 2687; (*b*) S. A. Tysoe, R. J. Morgan, A. D. Baker and T. C. Strekas, *J. Phys. Chem.*, 1993, **97**, 1707; (*c*) A. D. Baker, R. J. Morgan and T. C. Strekas, *J. Chem. Soc., Chem. Commun.*, 1992, 1099.

5 A. Yamagishi, *J. Phys. Chem.*, 1984, **88**, 5709; K. Naing, M. Takahashi, M. Taniguchi and A. Yamagishi, *J. Chem. Soc., Chem. Commun.*, 1993, 402.

6 (*a*) C. Hiort, B. Nordén and A. Rodger, *J. Am. Chem. Soc.*, 1990, **112**, 1971; (*b*) M. Eriksson, M. Leijon, C. Hiort, B. Nordén and A. Graslund, *Biochemistry*, 1994, **33**, 5031; (*c*) C. Hiort, P. Lincoln and B. Nordén, *J. Am. Chem. Soc.*, 1993, **115**, 3448.

7 (*a*) S. Satyanarayana, J. C. Dabrowiak and J. B. Chaires, *Biochemistry*, 1992, **31**, 9319; (*b*) S. Satyanarayana, J. C. Dabrowiak and J. B. Chaires, *Biochemistry*, 1993, **32**, 2573; (*c*) I. Haq, P. Lincoln, D. Suh, B. Norden, B. Z. Chowolhry and J. B. Chaires, *J. Am. Chem. Soc.*, 1995, **117**, 4788.

8 A. Kirsch-De Mesmaeker, G. Orellana, J. K. Barton and N. J. Turro, *Photochem. Photobiol.*, 1990, **52**, 461; G. Orellana, A. Kirsch-De Mesmaeker, J. K. Barton and N. J. Turro, *Photochem. Photobiol.*, 1991, **54**, 499; J. P. Lecomte, A. Kirsch-De Mesmaeker and G. Orellana, *J. Phys. Chem.*, 1994, **98**, 5382.

9 W. A. Kalsbeck and H. H. Thorp, *J. Am. Chem. Soc.*, 1993, **115**, 7146; D. H. Johnston, K. C. Glasgow and H. H. Thorp, *J. Am. Chem. Soc.*, 1995, **117**, 8933.

10 I. S. Haworth, A. H. Elcock, A. Rodger and W. G. Richards, *J. Biomol. Struct. Dynamics*, 1991, **9**, 553; I. S. Haworth, A. H. Elcock, J. Freeman, A. Rodger and W. G. Richards, *J. Biomol. Struct. Dynamics*, 1991, **9**, 23.

11 C. Sentagne, J. C. Chambron, J. P. Sauvage and N. Paillous, *J. Photochem. Photobiol. B: Biol.*, 1994, **26**, 165.

12 D. L. Carlson, D. H. Huchital, E. J. Mantilla, R. D. Sheardy and W. R. Murphy, *J. Am. Chem. Soc.*, 1993, **115**, 6424.

13 S. Mahaderan and M. Palaniandavar, *J. Inorg. Biochem.*, 1995, **59**, 161.

14 S. J. Lippard, P. J. Bond, K. C. Wu and W. R. Bauer, *Science*, 1976, **194**, 726; S. J. Lippard, *Acc. Chem. Res.*, 1978, **11**, 211; A. H.-J. Wang, J. Nathans, G. Van der Marel, J. H. Van Boom and A. Rich, *Nature* (*London*), 1978, **276**, 471; S. Sherman, D. Gibson, A. H.-J. Wang and S. J. Lippard, *Science*, 1985, **230**, 412; R. V. Gessner, G. J. Ouigley, A. H.-J. Wang, G. A. Van der Marel, J. H. Van Boom and A. Rich, *Biochemistry*, 1985, **24**, 237; S. E. Sherman and S. J. Lippard, *Chem. Rev.*, 1987, **87**, 1153; P. S. Ho, C. A. Frederick, D. Sael, A. H.-J. Wang and A. Rich, *J. Biomol. Struct. Dynamics*, 1987, **4**, 521; G. Admiraal, J. L. Vander Veer, R. A. G. De Graaff, J. H. J. Den Hartog and J. Reedijk, *J. Am. Chem. Soc.*, 1987, **109**, 592; J. Reedijk, A. M. J. Fichtinger-Schepman, A. T. van Oosterom and P. Van de Putte, *Struct. Bonding* (*Berlin*), 1987, **67**, 53; P. Umapathy, *Coord. Chem. Rev.*, 1989, **95**, 129.

15 J.-Z. Wu, L. Wang, G. Yang, L.-N. Ji, N. Katsaros and A. Koutsodimou, *Cryst. Res. Tech.*, 1996, **31**, 857.

16 B. P. Sullivan, D. J. Salmon and T. J. Meyer, *Inorg. Chem.*, 1989, **17**, 3334.

17 J. Marmur, *J. Mol. Biol.*, 1961, **3**, 208.

18 M. E. Reichmann, S. A. Rice, C. A. Thomas and P. Doty, *J. Am. Chem. Soc.*, 1954, **76**, 3047.

19 G. M. Sheldrick, SHELXTL PC, Siemens Analytical X-Ray Instruments Inc., Madison, WI, 1990.

20 D. P. Rillema, G. Allen, T. J. Meyer and D. C. Conrad, *Inorg. Chem.*, 1983, **22**, 1617.

21 E. Amouyal, A. Homsi, J.-C. Chambron and J.-P. Sauvage, *J. Chem. Soc., Dalton Trans.*, 1990, 1841.

22 (*a*) B. K. Ghosh and A. Chakravorty, *Coord. Chem. Rev.*, 1989, **95**, 239; (*b*) F. Brigelletti, A. Juris, V. Balzani, P. Belser and A. von Zelewsky, *Inorg. Chem.*, 1987, **26**, 4115; (*c*) Y. Fuchs, S. Lofters, T. Dieter, W. Shi, R. Morgan, T. C. Strekas, H. D. Gafney and A. D. Baker, *Inorg. Chem.*, 1987, **109**, 2691; (*d*) J. E. B. Johnson and R. R. Ruminski, *Inorg. Chim. Acta*, 1993, **208**, 231; (*e*) M. R. McDevitt, Y. Ru and A. W. Addison, *Transition Met. Chem.*, 1993, **18**, 197.

23 C. K. Johnson, ORTEP, Report ORNL-5138, Oak Ridge National Laboratory, Oak Ridge, TN, 1976.
24 D. P. Rillema, D. S. Jones and H. A. Levy, *J. Chem. Soc., Chem. Commun.*, 1979, 849; D. P. Rillema, D. S. Jones, C. Woods and H. A. Levy, *Inorg. Chem.*, 1992, **31**, 2935.
25 B.-H. Ye, X.-M. Chen, T.-X. Zeng and L.-N. Ji, *Inorg. Chim. Acta*, 1995, **240**, 11.
26 (*a*) D. S. Eggleston, K. A. Goldsby, D. J. Hodgson and T. J. Meyer, *Inorg. Chem.*, 1985, **24**, 4573; (*b*) M. A. Anderson, J. P. G. Richards, A. G. Stard, F. S. Stephens, R. S. Vagg and P. A. Williams, *Inorg. Chem.*, 1986, **25**, 4847; (*c*) R. H. Herber, G. Nan, J. A. Potenza, H. J. Scheegar and A. Boma, *Inorg. Chem.*, 1989, **28**, 938; (*d*) E. C. Constable, *Polyhedron*, 1989, **8**, 83; (*e*) P. Belser, A. von Zelewsky and M. Zehnder, *Inorg. Chem.*, 1987, **26**, 2370.
27 B. M. Goldstein, J. K. Barton and H. M. Berman, *Inorg. Chem.*, 1986, **25**, 842.
28 M. N. Ackermann and L. V. Interrante, *Inorg. Chem.*, 1984, **23**, 3904.
29 A. M. Pyle, M. Y. Chiang and J. K. Barton, *Inorg. Chem.*, 1990, **29**, 4887.
30 D. P. Rillema, G. Allen, T. J. Meyer and D. Conrad, *Inorg. Chem.*, 1983, **22**, 1617; D. P. Rillema, C. B. Blanton, R. J. Shaver, D. C. Jackman, M. Boldaji, S. Bundy, L. A. Worl and T. J. Meyer, *Inorg. Chem.*, 1992, **31**, 1600.

Received 29*th July* 1996; *Paper* 6/05269J